JOURNAL OF MATERIALS SCIENCE 26 (1991) 5848–5858

Toughening mechanism for a rubber-toughened epoxy resin with rubber/matrix interfacial modification

TENG KO CHEN*, YI HUNG JAN
Chemical Engineering Department, National Central University, Chung-Li, Taiwan 32054

For a rubber-toughened piperidine–DGEBA epoxy resin, the interface between the rubber particle and the epoxy resin matrix was modified by an epoxide end-capped carboxyl terminated butadiene and acrylonitrile random copolymer (CTBN). The end-capping epoxides used were a rigid diglycidyl ether of bisphenol-A (Epon 828), a short-chain flexible diglycidyl ether of propylene glycol (DER 736), and a long-chain flexible diglycidyl ether of propylene glycol (DER 732). The microstructures and the fracture behaviour of these rubber-modified epoxy resins were studied by transmission electron microscopy and scanning electron microscopy. Their thermal and mechanical properties were also investigated. In the rubber-modified epoxy resins, if the added CTBNs were end-capped by a flexible diglycidyl ether of propylene glycol (DER 732 or DER 736) before curing, the interfacial zone of the undeformed rubber particle, the degree of cavitation of the cavitated rubber particle on the fracture surface and the fracture energy of the toughened epoxy resin were all significantly increased. The toughening mechanism based on cavitation and localized shear yielding was considered and a mechanism for the interaction between cavitation and localized shear yielding that accounts for all the observed characteristics is proposed.

1. Introduction

Many efforts have been made to improve the toughness of a cured epoxy resin. The most successful method is the addition of some reactive liquid rubber, such as CTBN, a carboxyl-terminated butadiene–acrylonitrile random copolymer, to a liquid epoxy resin system [1–4]. The reactive liquid rubber is first dissolved in the liquid resin; as curing proceeds, the rubber precipitates out from the epoxy and forms a fine dispersion of rubber particles with diameters of a few micrometres or less. During the last two decades, improvement in epoxy toughness has been attributed to a number of fracture mechanisms, which included rubber tearing [5, 6], crazing [2–4], shear flow and crazing [7, 8]. Most of the mechanisms have given rise to a great deal of controversy. Recently, a fracture mechanism proposed with cavitation and shear yielding processes [9–11] has been identified and well-accepted in the literature [12–16]. This mechanism indicates that the greater crack resistance in the rubber-modified epoxy arises from the greater extent of energy-dissipating deformation occurring in the crack tip. The deformation includes two processes: cavitation at the particle/matrix interface, and multiple but localized plastic shear yielding in the adjacent matrix initiated by the stress concentration associated with rubber particles. Although both of these processes may be initiated once loading commences, the interaction between them serves to magnify the amount of shear yielding in the matrix. Thus it can be proposed that the particle/matrix interface will play an important role in the toughness of rubber-modified epoxy system. Unfortunately, the importance of the particle/matrix interface has been almost ignored in the early work [11]. If mentioned at all, it was restricted to the study of the interfacial bonding force [2, 17, 18]. Moreover, Kunz *et al.* [19] and Sayre *et al.* [20] have shown in their experimental studies that the interfacial region where segmental mixing has occurred, is less than 50 nm wide. Owing to the very narrow interfacial zone, they concluded that any property in the interfacial zone was not significant in the overall toughness. Because the mechanism of cavitation and shear yielding proposed that the toughening mechanism is initiated from the rubber/matrix interface, it is of greater interest to study further the property and size of the interface. In this work, CTBN was first end-capped with different kinds of epoxy monomers, including DER 732, DER 736 and Epon 828. These resins are distinguished by different molecular flexibility, chain length, and compatibility with the epoxy matrix. As a consequence of the compatibility between epoxy resin and CTBN, the chain ends of the CTBN may tend to concentrate at the interface. Thus, one

*Author to whom all correspondence should be addressed.

0022–2461/91 $03.00 + .12

may expect the interfacial zone of the modified CTBN rubber particles will result in different degrees of deformability and the zone size may also increase. Both variations may greatly influence the cavitation process and contribute to greater energy dissipation in the crack front.

2. Experimental procedure

2.1. Materials

The epoxy resin used to form the matrix phase was Epon 828, a diglycidyl ether of bisphenol-A (DGEBA). Three different epoxy monomers were used to modify the properties of the particle/matrix interface. The first was Epon 828, which is the same epoxy resin used for the matrix phase. The second was DER 736, which is a short-chain diglycidyl ether of propylene glycol (DGEPG) with an average degree of polymerization, $\bar{n} = 4$. The third was DER 732, which is also a DGEPG resin but with longer chain length of $\bar{n} = 9$. These interfacial modifiers are described by the structure formulae I–III.

Epon 828

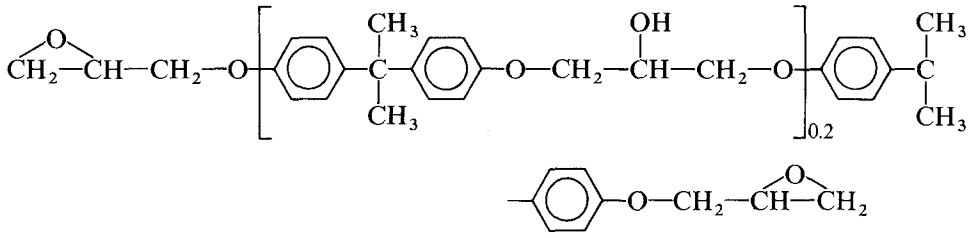

(I)

DER 736

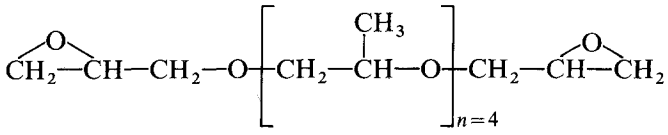

(II)

DER 732

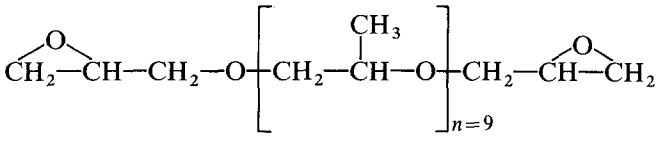

(III)

Some important properties of these interfacial modifiers are listed in Table I. The rubber used was a carboxyl terminated random copolymer of butadiene and acrylonitrile (Hycar CTBN1300X8). Some important properties of this rubber are listed in Table II. The curing agent was piperidine, a cycloaliphatic amine.

2.2. End-capping of CTBN

Each of the end-capping reagents (Epon 828, DER 736 or DER 732) was added to the liquid CTBN rubber in a three-neck flask blanketed with nitrogen. The formulations (Table III) were designed for the molar ratio of epoxide group to the carboxyl group of 2. The flask was heated in an oil bath with mechanical stirring for 4 h at 150 °C [5, 6, 21]. Under these conditions the end-capping reaction will be completed and each chain end of CTBN molecule will be capped by one end-capping epoxide. At the ends of these reactions, a small amount of the mixture was taken out for the analysis of the carboxyl content, the number average

TABLE I Properties of the interfacial modifiers

Property	Interfacial modifier		
	DER 732	DER 736	Epon 828
Epoxide equivalent weight	329	190	187
Solubility parameter	9.129	9.344	9.440
Specific gravity, 25/25 °C	1.060	1.140	1.160
Brookfield viscosity (cP) at 25 °C	55–100	30–60	11 000–14 000

molecular weight ($\bar{M}_n$) and the molecular weight distribution (MWD). The carboxyl content was determined by a titration method [21, 22]. $\bar{M}_n$ and MWD were determined by vapour pressure osmometry (Knauer, Model 1100) and gel permeation chromatography (Waters, type 440), respectively.

2.3. Manufacture of the rubber-modified epoxy resins

The formulations of all the rubber-toughened epoxy resins in this investigation are listed in Table IV. To prepare the modified interface, the CTBN rubber was first end-capped with different kinds of epoxides; to modify the matrix, the same quantity of modifying epoxide was added directly to the epoxy mixture. The rubber, with or without end-capping, was added to the epoxy mixture and heated to 65 °C in an oil bath which was further stirred until a homogeneous mixture was reached. The mixture was then removed to a vacuum oven and degassed until frothing stopped. When the mixture was cooled to room temperature, the piperidine was gently added to the mixture to minimize air entrapment. The rubber–epoxy mixture was then poured into a preheated glass mould, which was further removed to an air-circulated over for resin curing. The curing cycles for all the formulated epoxy resins were under the same conditions, i.e. cured at 120 °C for 16 h and, finally, allowed to cool slowly to room temperature. The experiments described below for microstructural and fracture studies were conducted using specimens obtained from these moulded resin plaques.

TABLE II Properties of CTBN1300X8

Property	CTBN1300X8
Acrylonitrile content (%)	17
Brookfield viscosity (cP) at 27 °C	125 000
Carboxyl content (%)	2.37
Molecular weight	3 500
Functionality	1.85
Solubility parameter	8.77
Specific gravity at 25 °C	0.948

2.4. Microstructural analysis

The microstructures of the cured epoxy materials were investigated by transmission electron microscopy (TEM), differential scanning calorimetry (DSC) and dynamic mechanical analysis (DMA). Specimens for TEM analysis were microtomed from materials which had been machined to square rods with each edge about 1 mm. Ultra-thin sections of the cured materials were obtained using an ultra-microtome (Reichert-Jung Ultracut-E) and a diamond knife (Micro Star, Standard Type) fixed at 50° angle. To avoid interference from particle curvature while examining the rubber particles, ultra-thin sections were microtomed to a thickness of less than 100 nm. For direct examination of the two-phase nature in a rubber-modified epoxy system, the ultra-thin sections were stained for 5 min in a tetrahydrofuran solution containing 1 wt/vol % osmium tetraoxide (OsO_4) as suggested by Riew and Smith [23]. The OsO_4 reacts with the unsaturated rubber to give a relatively electron-opaque region. The microscopy was conducted using a Hitachi H-600-3 TEM. Quantitative analysis of rubber-particle size distribution was based on the Schwartz–Saltykov method [24], which requires transmission electron micrographs containing at least a total of 100 rubber particles. The volume fraction of

TABLE III Compositions for the end-capped CTBN rubber

Designation for end-capped rubber	End-capping monomer	Amount of CTBN (wt/wt %)	Amount of end-capping epoxide (wt/wt%)	Molar ratio of CTBN to end-capping epoxide
R732	DER 732	74.2	25.8	1/2
R736	DER 736	83.3	16.7	1/2
R828	Epon 828	83.5	16.5	1/2

TABLE IV Formulations of the rubber-toughened epoxy resins[a]

Designation for epoxy resin	Amount of CTBN (p.h.r.)	Type of epoxide modifier	Amount of epoxide modifier (p.h.r.)	Location of modifying epoxide
E	0.0	–	–	–
E-R732	10.0	DER 732	3.48	interface
E-R736	10.0	DER 736	2.01	interface
E-R828	10.0	Epon 828	1.98	interface
E-M732	10.0	DER 732	3.48	matrix
E-M736	10.0	DER 736	2.01	matrix
E-M828	10.0	Epon 828	1.98	matrix

[a] The total resin content was fixed at 100 p.h.r for all the epoxy materials.

the rubbery phase was also calculated from the micrographs using the method suggested by Guy [25].

DSC analysis was conducted at a heating rate of 20 °C min^{-1} in a DuPont 9900 calorimeter and was operated over the temperature range − 100 to + 150 °C.

2.5. Tensile property measurement

The tensile tests were performed by using an Instron 1302 tensometer and an Instron 2620-602 extensometer. The dumb-bell specimens were cut from 3 mm resin plaques in accordance with descriptions in ASTM D638-64T. The crosshead speed of the tensometer was kept constant at 1 mm min^{-1}. The testing temperature was held at 25 °C.

2.6. Fracture energy measurement

In this investigation, the fracture toughness of the experimental materials was measured in terms of the critical strain energy release rate, G_{Ic}. This value was determined using a tapered double cantilever beam (TDCB) specimen which was originally developed by Mostovoy *et al.* [26]. These specimens were machined from 6 mm resin plaques in accordance with the description in Fig. 1. A sharp crack was formed at the base of the slot by carefully tapping a fresh razor blade in the base, thus causing a sharp crack to grow naturally for a short distance ahead of the razor blade. The advantage of using Mostovoy's specimens is mainly due to the recorded load which is independent of crack length. Therefore, the heights of all the load peak should be equal and each of them can be taken into account for calculating the G_{Ic} values [26]. The other advantage is that the G_{Ic} values can be easily calculated from the equation

$$G_{Ic} = 4P^2m/Ebb' \quad (1)$$

where P is the load required to propagate the crack, E is the Young's modulus, b is the specimen thickness, b' is the side groove thickness and m is a constant which depends on the specimen shape and has a value of 3.27 cm^{-1} in this investigation. The fracture energy test was conducted by an Instron 1302 tensometer with crossheads moving at 1 mm min^{-1}. The temperature for this test was held at 25 °C.

2.7. Fractography

The fracture surface was examined under a Hitachi S-750 scanning electron microscope at an accelerating voltage of 20 kV. Prior to examination, the fracture surface was coated with a thin evaporated layer of gold in order to improve conductivity of the examined fracture surface and prevent electron charging on them.

3. Results and discussion

3.1. End-capping of CTBN rubber

Three kinds of epoxy monomer, Epon 828, DER 736 and DER 732, with different solubility parameters,

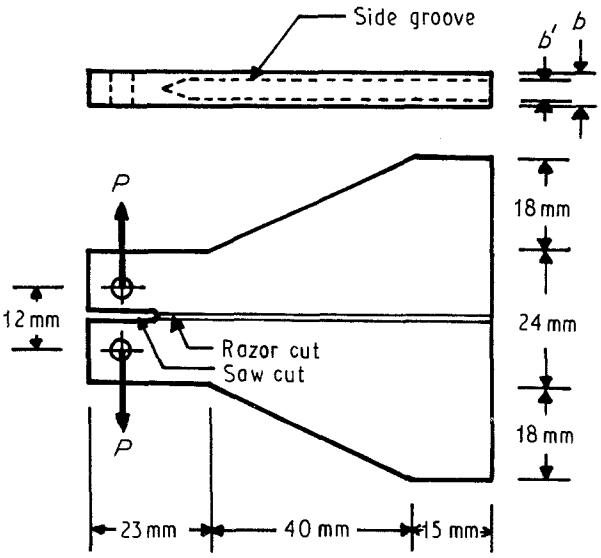

Figure 1 TDCB specimen for fracture energy studies.

TABLE V Number average molecular weight of the end-capped CTBN

Designation	$\bar{M}_n$	
	Exp.[a]	Theor.[b]
R732	4700	4700
R736	4400	4300
R828	4200	4200

[a] Obtained from vapour pressure osmometry.
[b] Calculated from the number average degree of polymerization [27].

molecular flexibility and chain length, were used to end-cap the CTBN rubber. All the end-capping reactions were carried out with a molar ratio of epoxide group to carboxyl group of 2. This molar ratio enabled both ends of the CTBN molecule to be capped with the epoxy monomers if the reaction was completed. The results from titration of carboxyl group concentration before and after end-capping reactions indicated the reactions were all completed. Infrared spectra also showed the same results, as observed from the disappearance of the characteristic carboxyl absorptions at 1710 and 3200 cm^{-1}, and the formation of characteristic ester absorption at 1737 cm^{-1}. The number average molecular weights ($\bar{M}_n$) obtained from vapour pressure osmometry for these end-capped products are listed in Table V. The values ranged from 4000–5000 and were around the values for one CTBN molecule end-capped with two Epon 828, DER 736 or DER 732 monomers, respectively. This result coincides with the theoretical calculation for the number average degree of polymerization, $\bar{X}_n$, according to the following equation [27]

$$\bar{X}_n = (1 + r)/(1 + r - 2rp) \quad (2)$$

where r is the stoichiometric imbalance and p is the extent of the reaction. The molecular weight distributions obtained from GPC for these end-capped products are slightly biased to the higher molecular

weight region, but their shapes remain the same as that for the original CTBN rubber. Both $\bar{M}_n$ and MWD results indicated that there is no extensive degree of chain extension during the end-capping reaction.

3.2. TEM studies for rubber-particle morphology

According to a recent review by Kinloch [11], the microstructural features which might affect the toughness of a rubber-modified epoxy resin include the precipitated rubber volume fraction, rubber-particle size, rubber-particle size distribution, adhesion across the particle/matrix interface, morphology of the dispersed phase and the glass transition temperature of the dispersed phase. In many studies, several features may change simultaneously; an individual result is often inconclusive. Our intention here was to study the effect of the particle/matrix interface. Therefore, all the features which might influence the mechanical properties in this study were carefully isolated and examined.

The transmission electron micrographs, at × 5000 magnification, for each rubber-toughened systems are shown in Fig. 2a–f. By using these micrographs and the Schwartz–Saltykov quantitative calculation [24], the particle size distribution, average particle diameter, and particle number per unit volume for each rubber-toughened epoxy system can be determined. The particle size distributions in Fig. 3a–f reveal mono-dispersed particle distribution with all the particle sizes ranging from 1–3 μm per 1000 μm^3. The average particle diameter and particle number are listed in Table VI. The average particle diameters in each system are all about 2 μm. The particle number per 1000 μm^3 in each system all fall within the range 20–25. The similar morphology of the dispersed phase in each system may be explained as follows. The end-capped epoxides have solubility parameters at 9.44 for Epon 828, at 9.94 for DER 736 and at 9.13 for DER 732, respectively. The difference in solubility parameters is not too significant. In addition, the weight fractions of the end-capping epoxides were all less than 20 wt/wt % of their modified CTBNs rubber. Therefore, it is reasonable to expect the modified CTBNs to behave similarly during curing and to be precipitated into rubber particles with similar morphology.

Another important feature of the dispersed phase is the volume fraction, V_p. It is defined as the fraction of material enclosed within the boundaries of the rubber particles, including not only the rubber itself, but also any resin trapped in the particles [7]. Several studies in the literature [5, 7, 10, 12, 16, 19] had concluded that the toughness of a rubber-modified epoxy resin increases as V_p is increased. V_p for each toughening system is listed in Table VII. It is revealed that the values of V_p are about the same and are very close to the initial volume fraction of CTBN. This observation simplifies the system under investigation by excluding the complexity associated with the variation of V_p.

To deal with the modification of the interfacial zone, some flexible DGEPGs which are compatible with the matrix resin were end-capped on to the CTBN rubber with the expectation that DGEPG will anchor to the interface and will plasticize and enlarge the interfacial zone. The results shown in Fig. 4a–c confirm this expectation. By observing the morphology of the particle/matrix interface, there is a zone of interfacial mixing. This zone is observed through the presence of some OsO_4-stained CTBN rubber. The following reasons may be given for the formation of this interfacial segmental mixing. The chain ends of these end-capped CTBN rubbers are epoxide groups, which are reactive to the piperidine curing agent. During the phase separation process, both ends of the modified CTBN rubber are likely to react with the interfacial DGEBA. In addition, the solubility parameters of these end-capping segments are higher than that of the CTBN rubber but close to that of the DGEBA resin. These end-capping segments may, therefore, concentrate at the interfacial zone. Moreover, in accordance with Manzione and Gillham's study [28], which indicated that the mobility of a molecule is proportional to its diffusivity, a flexible segment in the chain end may have higher diffusivity and may pull some CTBN deeper into the adjacent matrix phase before gelation occurs. Fig. 4a–c are micrographs taken at very high magnification (× 40 000) for toughening systems with CTBN end-capped by DER 732, DER 736, and Epon 828, respectively. The degree of interfacial mixing is very significant and reveals a decreasing order with DER 732 > DER 736 > Epon 828. From these results, it is realized that end-capping of CTBN rubber may be an effective way to modify the properties of the interfacial zone, but the end-capping epoxide should be carefully selected. In this piperidine–DGEBA epoxy system, the most effective end-capping epoxide was DER 732. In order to elucidate more clearly the effect of the modifiers, the same amount of modifier was directly blended into the resin mixture instead of capping at the CTBN chain end. Fig. 4d–f are micrographs for systems prepared by directly formulating the modifiers DER 732, DER 736, and Epon 828, respectively, into the resin mixture. As shown in these micrographs, the interfacial mixing is not significant and limited to a thickness of less than 50 nm. This is in agreement with Sayre *et al.*'s [20] observation by EDEX analysis. The modifiers thus added were not concentrated at the particle/matrix interface and were more likely distributed in the matrix phase.

3.3. The matrix property

In this investigation, the matrix property is represented by the glass transition temperatures, T_g, of matrix phase. These T_g values are shown in Table VIII. No matter what flexible epoxy monomer was used to end-cap the CTBN rubber or was directly blended into the resin mixture, there is no significant difference in the matrix T_g compared with that for the unmodified epoxy resin. The reasons are easy to comprehend. For the system with end-capped DER 732, DER 732 is located in the rubber/matrix interfacial zone, which

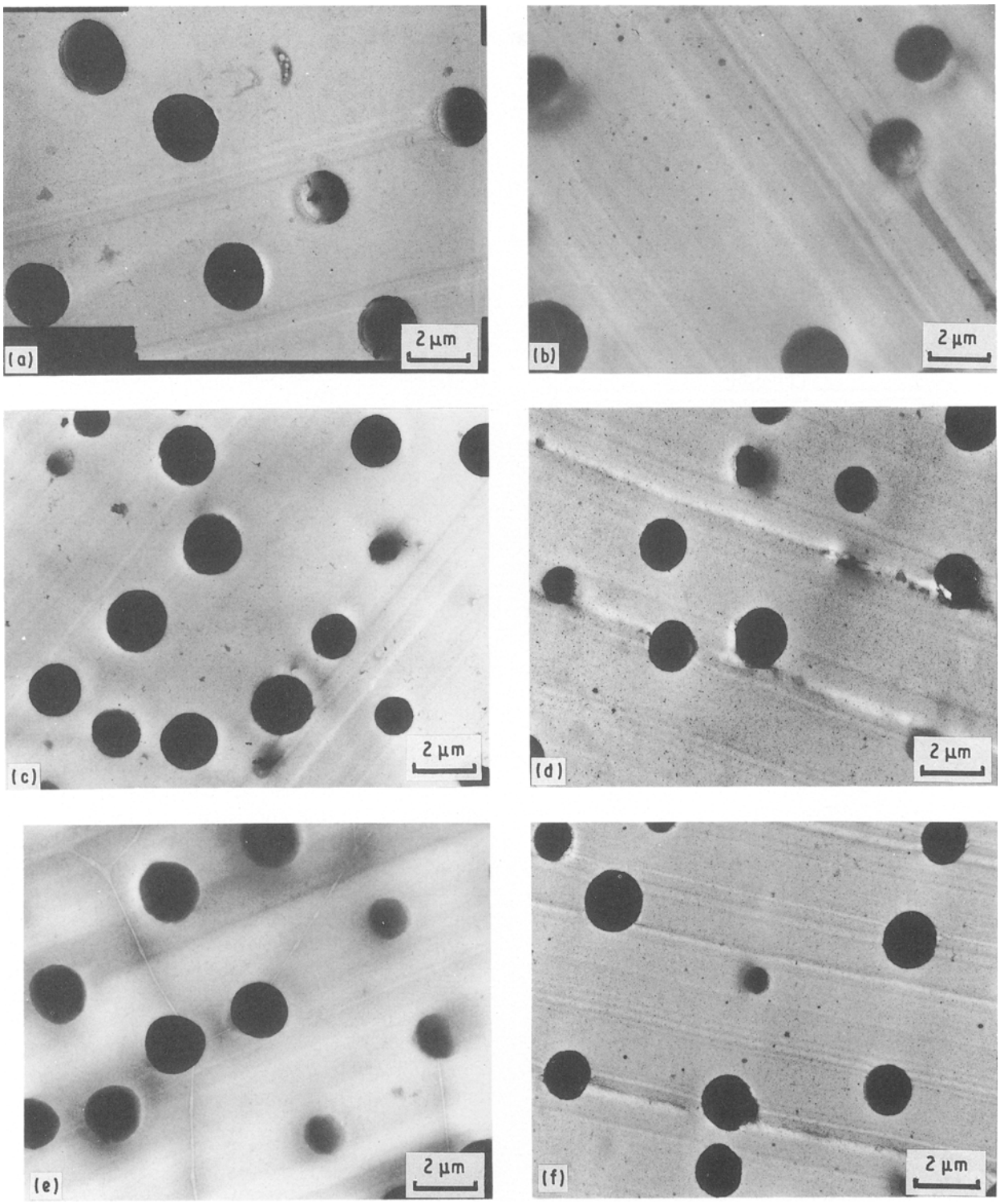

Figure 2 Transmission electron micrographs of microtomed sections for (a) E-R732, (b) E-R736, (c) E-R828, (d) E-M732, (e) E-M736 and (f) E-M828.

TABLE VI Rubbery phase morphology of the toughened epoxy resins

Designation	Distribution type	Particle diameter (μm)	Particle number (10^{-3} μm^3)
E-R732	Mono-dispersed	2.10	22.5
E-R736	Mono-dispersed	1.82	25.7
E-R828	Mono-dispersed	2.05	19.8
E-M732	Mono-dispersed	2.02	23.7
E-M736	Mono-dispersed	1.87	24.8
E-M828	Mono-dispersed	1.89	25.0

TABLE VII Rubber volume fractions for the toughened epoxy resins

Designation	Volume fraction of precipitated rubber (%)	Volume fraction of initially added rubber (%)
E-R732	11.6	11.3
E-R736	9.0	11.3
E-R828	10.3	11.3
E-M732	11.2	11.3
E-M736	9.5	11.4
E-M828	9.8	11.4

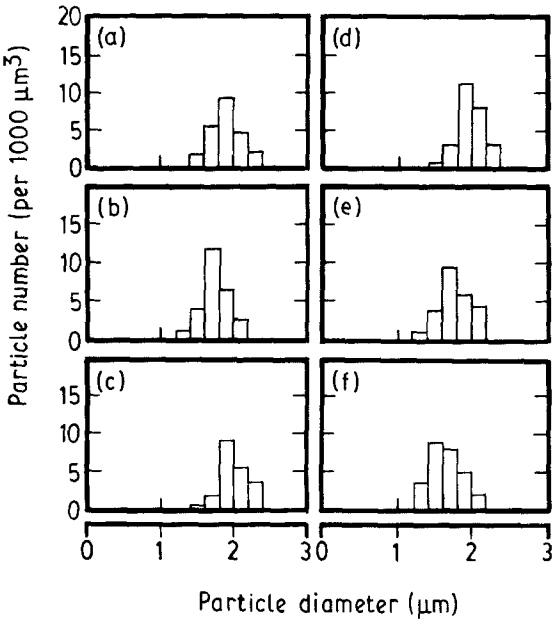

Figure 3 Particle size distributions for (a) E-R732, (b) E-R736, (c) E-R828, (d) E-M732, (e) E-M736 and (f) E-M828.

would not affect the matrix property. For the system with directly blended DER 732, most of the DER 732 would go into the matrix phase. However, the amount of DER 732 used is less than 3.5 wt/wt % of the amount of DGEBA in the matrix phase. The amount of added DER 732 is thus too small to affect the matrix property.

3.4. Mechanical properties

In the discussion so far, features affecting the mechanical properties of the rubber-modified epoxy resin as reviewed by Kinloch [11] have all been examined. With the exception of the matrix/particle interface which was found to vary greatly, the other features do not seem to change to an extent large enough to influence the mechanical properties of a rubber-toughened epoxy resin. The relationship between the interfacial zone properties and the mechanical properties is investigated below.

3.4.1. Tensile properties

The tensile stress and tensile modulus for each system are listed in Table IX. It is clearly shown that these two properties remain almost constant in all the rubber-toughened epoxy resins. All the tensile stresses lie in the range 56–59 MPa and the tensile moduli in the range 2.0–2.3 GPa. The constancy of the tensile stress and the modulus indicates that they are only affected by the matrix property and the precipitated rubber volume fraction. Previous discussion indicated that both of the factors remain very constant in each toughened system.

3.4.2. Fracture energy

The fracture energy, G_{Ic}, was determined from the TDCB specimens and calculated by using Equation 1

TABLE VIII Glass transition temperature for the toughened epoxy resins

Designation	T_g of matrix (°C)
E	89.5
E-R732	89.5
E-R736	91.2
E-R828	91.0
E-M732	89.5
E-M736	89.7
E-M828	91.5

TABLE IX Tensile properties for the toughened epoxy resins

Designation	Tensile stress (MPa)	Tensile modulus (GPa)
E	75.3	2.4
E-R732	56.0	2.0
E-R736	56.8	2.2
E-R828	57.4	2.2
E-M732	56.2	2.3
E-M736	56.8	2.1
E-M828	58.9	2.1

[25]. The results for all the toughened epoxy resins are plotted in Fig. 5. For the toughened epoxy resin with non-end-capped CTBN, the fracture energies were not improved further and remained at a constant value around 1400 J m^{-2}, which is about the same value for the conventional CTBN/DGEBA/piperidine toughening system. For the end-capped CTBN toughened epoxy resins, the fracture energies were greatly increased and the increment depended on the type of chain end modifier. The resulting G_{Ic}s of the toughened epoxy resins were 1400, 1940 and 3300 J m^{-2}, for the resins with CTBN modified by Epon 828, DER 736 and DER 732, respectively. The increasing tendency for the G_{Ic}s follows the extent of segmental mixing in the interfacial region which was examined by TEM and is shown in Fig. 4. A wider and more deformable interfacial zone clearly plays an important role in the toughness of the epoxy resin.

3.5. Relationship between the interfacial zone properties and fracture mechanism

Because cavitation in the rubber particle and shear yielding in the matrix are well-established toughening processes [9–16], the effect of the interfacial zone on those processes will be discussed further. Based on this toughening mechanism, the degree of cavitation as a result of stress concentration and triaxial tension in the rubber/matrix interface will decrease the constraint on the adjacent matrix [10, 11]. Because the yield stress depends on the degree of constraint, yield stress in many local areas throughout the crack tip region will also be reduced. This promotes extensive shear-yielding in the matrix [10, 11]. It is the creation of this plastic deformation that is the principal toughening mechanism. With this basic concept, we first emphasize the issue of the degree of cavitation which

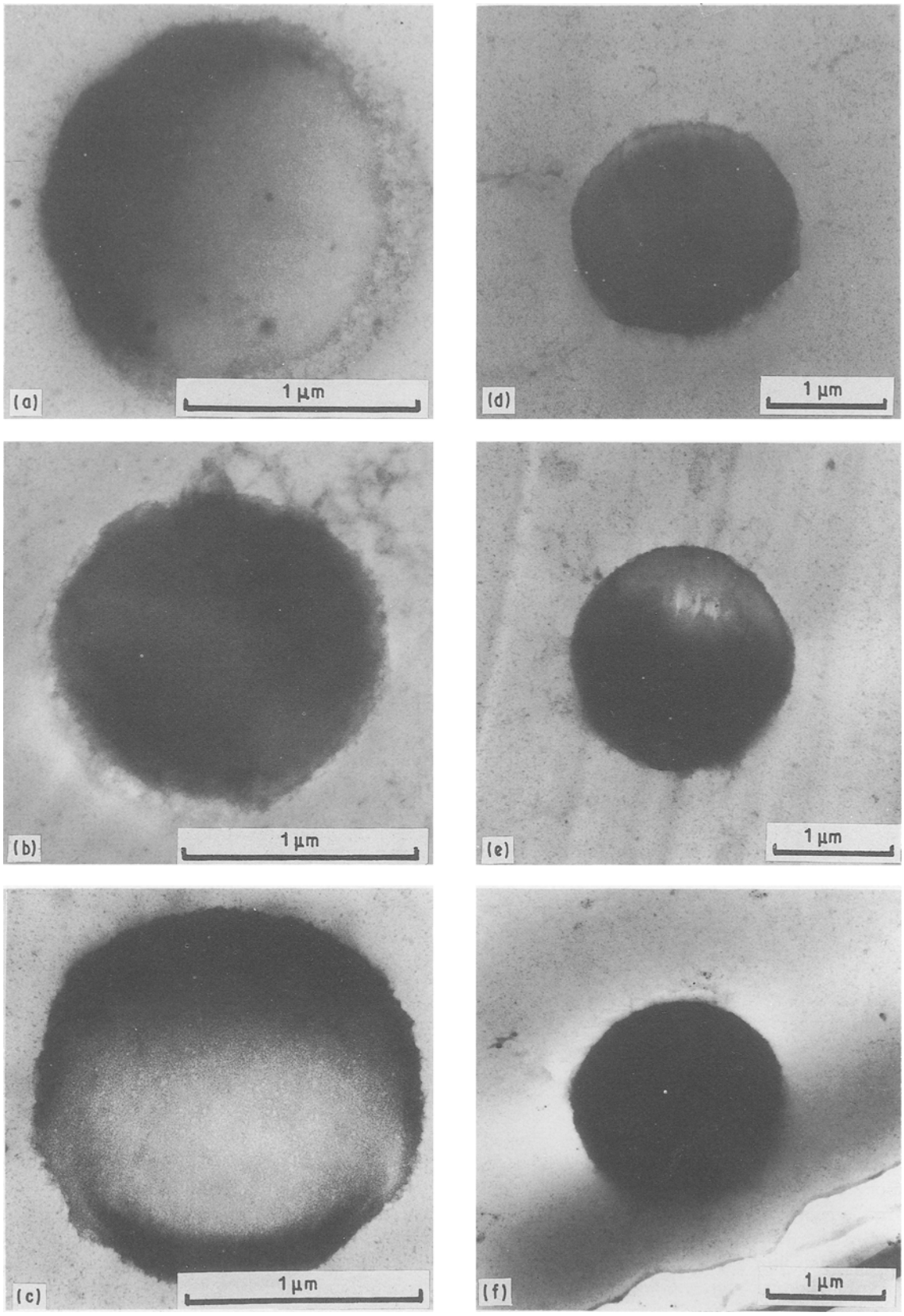

Figure 4 Higher magnification transmission electron micrographs of the microtomed sections in Fig. 2. (a) E-R732, (b) E-R736, (c) E-R828, (d) E-M732, (e) E-M736, (f) E-M828.

can be measured [13] by comparing the diameter of the cavities on a fracture surface with the diameter of the undeformed rubber particles in the matrix by using SEM and TEM. The cavity diameter is measured directly from scanning electron micrographs by assuming that the particles were broken on equatorial planes by the crack front, due to the stress concentration on these planes [29]. The diameter of the undeformed particles was calculated from the transmission electron micrographs as mentioned in Section 3.2. In general, the diameter of the cavity is larger than the diameter of the undeformed particles [10, 13] and the

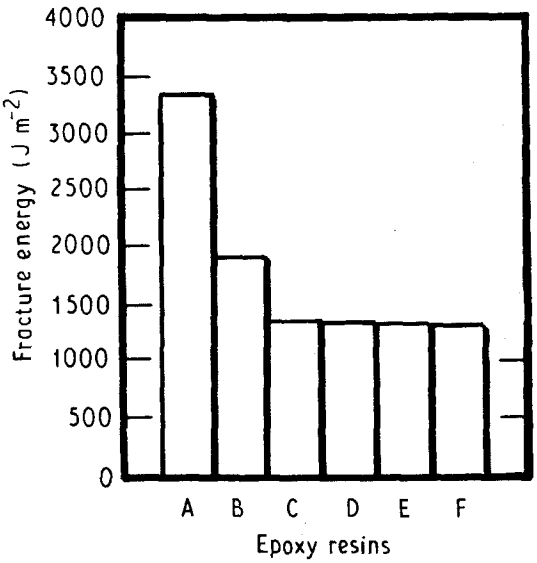

Figure 5 Fracture energy of the toughened epoxy resins. A, E-R732; B, E-R736; C, E-R828; D, E-M732; E, E-M736; F, E-M828.

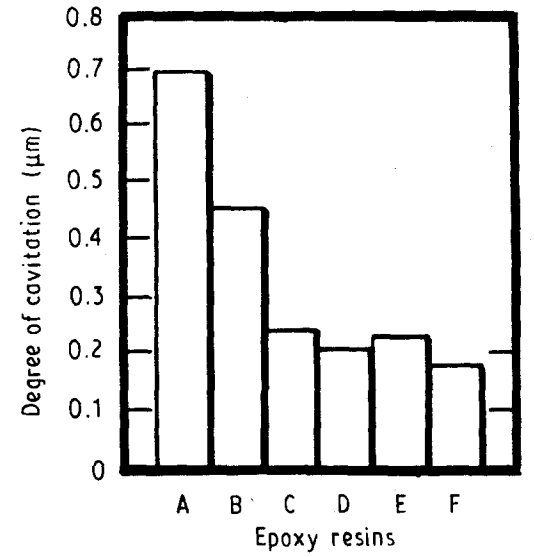

Figure 6 Degree of cavitation on fracture surface of the toughened epoxy resins. For key, see Fig. 5.

difference between these two diameters is considered to be the degree of cavitation occurring while the crack proceeds. Fig. 6 shows the experimental results of the degree of cavitation in each toughened epoxy resin. In the resins where the modifying epoxides were homogeneously distributed in the epoxy matrix, the degrees of cavitation are all about 0.2 μm, which is equal to that for the conventional CTBN/DGEBA/piperidine toughening system. In the systems where the modifying epoxides were end-capped on CTBN, the degree of cavitation varied greatly and the variation depended on the type of chain-end modifier. Among these chain-end modifiers, the degrees of cavitation are 0.2, 0.5 and 0.7 μm for modification with Epon 828, DER 736 and DER 732, respectively. The increasing tendency of the degree of cavitation also parallels the width of the interfacial zone, as shown in Fig. 4. This parallel tendency ascertains our original conjecture in Section 3.4.2, where we proposed that a more

TABLE X Size of stress whitening zone on the fracture surface of the toughened epoxy resins

Designation	Length of stress whitening zone (mm)	Depth of stress whitening zone (mm)
E-R732	2.2	1.6
E-R736	2.0	1.7
E-R828	1.9	1.6
E-M732	2.0	1.6
E-M736	2.1	1.4
E-M828	2.2	1.5

deformable and wider interfacial zone would result in a higher degree of cavitation and a higher fracture energy.

The other energy dissipation process in the current fracture mechanism is the localized plastic shear yielding in between rubber particles. A quantitative analysis of localized shear yielding is difficult to measure [11]. Based on a hypothesis given by Yee and Pearson [13], the formation of the localized shear yielding (i.e. the shear band) will cause the plastic zone to grow further ahead of the crack tip. Therefore, the maximal size of the plastic zone as shown by the stress whitening zone on the fracture surface should correlate to the maximal degree of localized shear yielding. The size of the stress whitening zone is identified by the length and depth of this zone, which were measured under an optical magnifier and are shown in Table X. The length was measured directly from the fracture surface of the stress whitening region. The depth was measured from a plane perpendicular to the fracture surface of the stress whitening region. This plane is made by grinding the fractured specimen to the central portion. Results from Table X indicate that the sizes of the stress whitening zones are all the same in this investigation. Furthermore, from visual inspection of the stress whitening zones, the degree of whiteness was found to correlate well with the fracture energy. As our measurements were done at a constant extension rate and temperature, the sizes of the stress whitening zones were all constant, but the fracture energy values were increased only with increasing degree of cavitation. These phenomena agree with Kinloch *et al.*'s experimental finding [10] where they indicated that the size of the stress whitening zone ahead of the crack tip correlates very well with the corresponding G_{Ic} values which were measured under varying extension rate and temperature. It may be reasonable to propose that, for a particular toughened epoxy resin fractured at a given extension rate and a given testing temperature, the localized shear yielding and the plastic flow of the matrix may have a characteristic maximum, and any further energy dissipation beyond this maximum may arise, if possible, simply from further cavitation. The modification on the rubber/matrix interfacial zone makes further cavitation possible. Thus, the extra improvement in fracture energy in this study in comparison with the fracture energy in a conventional rubber-toughened epoxy resin, may simply arise from the the higher degree of cavitation.

Theoretical model calculations showed that the cavitation reduces the octahedral shear stress to yield [4] and the cavities grow and promote the formation of localized plastic shear yielding between voids [4, 12, 30]. Localized shear deformation is enhanced in such a voidy solid [10, 12, 30, 31]. All these theoretical predictions were also made by Kinloch *et al.* [10] and Yee and Pearson [12, 13] in proposing the current fracture mechanism. Unfortunately, there is a lack of direct evidence for the above predictions. According to our experimental findings, the increase in the degree of cavitation from 0.2 μm up to 0.7 μm does not show any enhancement in the localized shear deformation. This contradiction clearly violates the above prediction. Although the cavitation may precede localized shear yielding in releasing bulk strain energy and even enhancing the degree of localized shear yielding in the early stage of crack arrest, our argument for this contradiction is that the growth of cavitation can only initiate the localized shear yielding. During the whole course of fracturing, the cavity diameter was found to increase at a small fraction of the original particle diameter. The characteristic value (maximum) of localized shear yielding may not be affected too much by cavitation growth. Therefore, in the later stage of crack arrest, the localized shear yielding may counteract the growth of cavitation. The degree of cavitation will finally proceed to an extent that meets the characteristic maximum in localized shear yielding. The maximum degree of cavitation will, finally, depend on the ease of cavitation growth. The DER 732 modified interfacial zone in this study indicates the ease for the cavitation to grow.

4. Conclusion

For a rubber-toughened piperidine–DGEBA epoxy resin, the interface between the rubber particle and the epoxy resin matrix was modified by an epoxide end-capped CTBN. The end-capping epoxides used were short-chain rigid DGEBA (Epon 828), a short-chain flexible DGEPG (DER 736) and a long-chain flexible DGEPG (DER 732). They were designed to anchor at the interface between the rubber particle and the epoxy matrix. TEM studies clearly identified a significant degree of interfacial mixing in the particle/matrix interface. Interfacial mixing increases as the end-capped epoxide changes from Epon 828, DER 736 to DER 732. The degree of rubber cavitation studied by combining TEM and SEM examination also identified a similar increasing trend. The fracture energies measured are significantly increased with the same trends, but the size of the stress whitening zone, as shown on the fracture surface, remains quite constant. All these results indicate that for a particular toughened epoxy resin fractured at a given extension rate and at a given testing temperature, the localized shear yielding and the plastic flow of the matrix may have a characteristic maximum. Any further energy dissipation beyond this maximum may arise, if possible, simply from further cavitation. The modification of the particle/matrix interface makes further cavitation possible.

The characteristic maximum in the localized shear yielding has led to a toughening mechanism that accounts for the interaction between the rubber cavitation and the localized shear yielding. Although the cavitation may precede localized shear yielding in releasing the bulk strain energy and even enhance the degree of localized shear yielding in the early stage of crack arrest, in the final stage of crack arrest, the localized shear yielding may counteract the degree of cavitation. The degree of cavitation will finally grow to an extent that meets the characteristic maximum in localized shear yielding. The maximum degree of cavitation will finally depend on the ease of cavitation growth.

Acknowledgement

This research was supported by the National Science Council, Taiwan, under Grant NSC 79-0405-E008-01.

References

1. E. H. ROWE, A. R. SIEBERT and R. S. DRAKE, *Mod. Plastics* **47** (1970) 110.
2. C. K. RIEW, E. H. ROWE and A. R. SIEBERT, in "Advances in Chemistry Series, No. 154. Toughness and Brittleness of Plastics" (ACS, Washington, 1976) p. 326.
3. J. N. SULTAN, R. C. LAIBLE and F. J. McGARRY, *J. Appl. Polym. Sci.* **6** (1971) 127.
4. J. N. SULTAN and F. J. McGARRY, *Polym. Engng Sci.* **13** (1973) 29.
5. S. KUNZ-DOUGLASS, P. W. R. BEAUMONT and M. F. ASHBY, *J. Mater. Sci.* **15** (1980) 1109.
6. S. C. KUNZ and P. W. R. BEAUMONT, *ibid.* **16** (1981) 3141.
7. C. B. BUCKNALL and Y. YOSHII, *Brit. Polym. J.* **10** (1978) 53.
8. C. B. BUCKNALL, "Toughened Plastics" (Applied Science, London, 1977).
9. W. D. BASCOM, R. Y. TONG, R. J. MOULTON, C. K. RIEW and A. R. SIEBERT, *J. Mater. Sci.* **16** (1981) 2657.
10. A. J. KINLOCH, S. J. SHAW, D. A. TOD and D. L. HUNSTON, *Polymer* **24** (1983) 1341.
11. A. J. KINLOCH, in "Structural Adhesives: Developments in Resins and Primers" (Elsevier Applied Science, London, 1986) p. 127.
12. A. F. YEE and R. A. PEARSON, *J. Mater. Sci.* **21** (1986) 2462.
13. *Idem, ibid.* **21** (1986) 2475.
14. A. J. KINLOCH, C. A. FINCH and S. HASHEMI, *Polym. Commun.* **28** (1987) 322.
15. R. A. PEARSON and A. F. YEE, *J. Mater. Sci.* **24** (1989) 2571.
16. A. J. KINLOCH and D. L. HUNSTON, *J. Mater. Sci. Lett.* **6** (1987) 131.
17. L. C. CHAN, J. K. GILLHAM, A. J. KINLOCH and S. J. SHAW, in "Rubber Modified Thermoset Resins", no. 208 (ACS, Washington, 1984) p. 261.
18. G. A. CROSBIE and M. G. PHILLIPS, *J. Mater. Sci.* **20** (1985) 182.
19. S. C. KUNZ, J. A. SAYRE and R. A. ASSINK, *Polymer* **23** (1982) 1897.
20. J. A. SAYRE, R. A. ASSINK and R. R. LAGASSE, *ibid.* **22** (1981) 87.
21. Y. D. LEE, S. K. WANG and W. K. CHIN, *J. Appl. Polym. Sci.* **32** (1986) 631.
22. S. GAZIT and J. P. BELL, *Amer. Chem. Soc. Org. Coatings Plast. Chem.* **46** (1982) 401.
23. C. K. RIEW and R. W. SMITH, *J. Polym. Sci. A1* **1** (1971) 2739.
24. E. E. UNDERWOOD, "Quantitative Sterology" (Addison-Wesley, Reading, MA, 1970) p. 109.

25. A. G. GUY, "Introduction to Material Science" (McGraw-Hill, New York, 1970).
26. S. MOSTOVOY, P. B. CRSLEY and E. J. RIPLING, *J. Mater.* **2** (1967) 661.
27. G. ODIAN, "Principle of Polymerization" (McGraw-Hill, New York, 1970).
28. L. T. MANZIONE and J. K. GILLHAM, *J. Appl. Polym. Sci.* **26** (1981) 889.
29. E. BUTTA, G. LEVITA, A. MARCHETTI and A. LAZZERI, *Polym. Engng Sci.* **26** (1986) 63.
30. H. YAMAMOTO, *Int. J. Fract.* **14** (1978) 347.
31. V. TVERGAARD, *ibid.* **17** (1981) 389.

Received 3 August 1990
and accepted 12 February 1991